Applied Acoustics 175 (2021) 107821

Contents lists available at ScienceDirect

Applied Acoustics

journal homepage: www.elsevier.com/locate/apacoust

Impact force excitation generated by an ISO tapping machine on wooden floors

Jesse Lietzén [a,*], Juha Miettinen [b], Mikko Kylliäinen [a], Sami Pajunen [a]

[a] Tampere University, Faculty of Built Environment, Civil Engineering, Hervanta Campus, P.O. Box 600, 33014 Tampere University, Tampere, Finland
[b] Tampere University, Faculty of Engineering and Natural Sciences, Material Sciences and Environmental Engineering, Hervanta Campus, P.O. Box 589, 33014 Tampere University, Tampere, Finland

ARTICLE INFO

Article history:
Received 24 June 2020
Received in revised form 8 October 2020
Accepted 25 November 2020

Keywords:
Impact sound insulation
Impact force
Tapping machine
Wooden floor

ABSTRACT

Prediction of the impact sound insulation of wooden floors requires information of the excitation forces driving the structure. According to earlier research, it is evident, that the impact force generated by the ISO tapping machine on the wooden floors is different than on bare concrete floors. However, only a few measurement results of the force have been shown in the literature. The purpose of our study was to experimentally determine the impact force excitation with an instrumented ISO tapping machine on a large range of wooden floors. One of the hammers of the tapping machine was equipped with both force and acceleration sensors. The hammer itself was modified to fulfil the requirements for the tapping machine presented in the standards ISO 10140-5 and ISO 16283-2. Based on the measured force signals, force spectra and impulses exerted by the instrumented hammer were determined. According to the results, differences between the force spectra on the wooden floors were prominent in the frequencies above 500 Hz. In the low-frequency range, the variation of the driving force corresponded to a level difference of more than 3 dB. In addition, the results showed that the process of excitation was not transient for the structures studied. Thus, the vibration of the measured wooden floors did not seem to influence the impact force. The findings of this paper are of very high importance for those developing mathematical calculation tools to predict the impact sound insulation of wooden floors.
© 2020 The Authors. Published by Elsevier Ltd. This is an open access article under the CC BY-NC-ND license (http://creativecommons.org/licenses/by-nc-nd/4.0/).

1. Introduction

The conventional and the most used standard impact sound source is the ISO standard tapping machine (presented in the standards ISO 10140-5 [1] and ISO 16283-2 [2]). The apparatus consists of five steel hammers, which are repeatedly dropped one at the time on the floor two times per second, thus resulting in a total repetition rate of 10 Hz. Hence, the tapping machine generates a quasi-stationary impact force excitation to the surface of the floor. The use of alternative sound sources has not become a common practice at least in Europe and the ISO tapping machine will most probably remain as the primary impact sound source [3]. Therefore, only the impact force excitation generated by the ISO tapping machine is studied in this paper.

Interaction between the tapping machine and the floor structure, i.e. the manner how the hammers hit the floor, depends on the type of the floor [4]. Since the tapping machine repeatedly drops its five hammers freely on to the surface of the floor, the force and the sound power input into the floor depends on the behaviour of the structure under the hammers. The peak impact force the apparatus produces is at its highest when the hammers hit a rigid and heavy structure, whereas it can be significantly lower when the structure under the hammers is elastic or when the surface structure of the floor is resilient, cf. [4]. These issues have also an effect on the length of the force pulses as well as on the spectrum of the impact force [4,5]. Due to these effects, it is obvious that the impact force excitation of lightweight structures differs from the force on a bare concrete structure.

Several models describing the impact force excitation of the floors generated by the ISO tapping machine have been presented in the literature [4,6–14]. A comparison between some of the models can be found for example in ref. [11]. Despite the models, only a few measurement results of the force have been shown in the literature. The studies conducted by Gudmundsson [15], Rabold et al. [11] and Olsson and Linderholt [16] distinguished some fundamental differences of the impact force generated by the ISO tapping machine on different floors. Furthermore, Jeon et al. [17] attempted to characterise the force input of different impact sources, and Amiryarahmadi et al. [18] compared the measured force spectrum

* Corresponding author.
E-mail address: jesse.lietzen@tuni.fi (J. Lietzén).

https://doi.org/10.1016/j.apacoust.2020.107821
0003-682X/© 2020 The Authors. Published by Elsevier Ltd.
This is an open access article under the CC BY-NC-ND license (http://creativecommons.org/licenses/by-nc-nd/4.0/).

generated by the tapping machine with the force spectrum caused by walking.

Apart from the study of Gudmundsson [15], measurement results of the impact force on different floor structures caused by ISO tapping machine have been presented only for a few floor structures. One reason for this is probably the tedious measurement setups. Secondly, the amplitude spectrum of the impact force generated by a single hammer blow of the hammer of the ISO tapping machine on bare concrete structures can often be considered rather constant [11,15]. Thus, there has probably been a minor need for investigating the impact force in the countries having buildings made mainly out of concrete. However, the force spectrum depends on the type of the floor as discussed above. Hence, more information of the impact force is required in order to understand better the behaviour of the tapping machine on lightweight structures. This is of particular importance for the acoustical engineers developing mathematical calculation tools applicable for the evaluation of the impact sound insulation of the wooden floors. One possibility to measure the impact force is to modify the hammers of the tapping machine.

In this study, the impact force excitation was measured with an instrumented tapping machine. The objective of the research was to study experimentally the spectrum and the impulse of the impact force excitation generated by the ISO tapping on wooden floors. The study included measurements for a large range of wooden floors with conventional floor coverings. Moreover, the aim was to study how the impact force was affected by the source position, the surface structures and the load-bearing structures. Additionally, the time dependency of the impact force excitation was discussed, referring to the requirements for the generation of sound field presented in the standards [1,2].

2. Methods

2.1. Excitation generated by the hammers of the ISO tapping machine

The drop height of the hammers of the ISO tapping machine is 40 mm and the mass of each hammer is 500 g. The full requirements for the ISO tapping machine are presented in the standards [1,2] which state, e.g. that the velocity of a hammer at impact v_0 shall be 0.886 m/s ± 0.022 m/s. This arises from the maximum permitted deviation of the mass of each hammer (12 g). Nevertheless, the impact force excitation cannot be generalized for all floor systems.

The formulation of the impact force excitation generated by the ISO tapping machine can be found from several sources in literature (see e.g. [4,5,8,11,12]). Here the formulation follows the presentation given by Brunskog and Hammer [4,19], where a two-sided representation of the spectrum of the force was used. The model considers a single hammer, but the excitation generated by every hammer could be formulated from this following the work of Wittstock [12].

The excitation force generated by the ISO tapping machine can be regarded as an infinite time series of separate force pulses $F(t)$ [4]. The length of the period T_r between the pulses for a single hammer is 0.5 s and the repetition rate $f_r = 1/T_r = 2$ Hz. Thus, the time history of the force pulse array $F_R(t)$ is a periodic signal and it can be represented by a two-sided complex Fourier series [4]

$$F_R(t) = \sum_{n=-\infty}^{\infty} F(t - nT_r) = \sum_{n=-\infty}^{\infty} F_n e^{i2\pi nt/T_r}, \tag{1}$$

where $i = \sqrt{-1}$ represents the imaginary unit and F_n is the amplitude of the discrete frequency components as follows

$$F_n = \frac{1}{T_r}\int_0^{T_r} F(t) e^{-\frac{i2\pi nt}{T_r}} dt. \tag{2}$$

The Fourier spectrum of the time history of the force is a tonal spectrum [4]

$$F_R(f) = \sum_{n=-\infty}^{\infty} F_n \delta(f - nf_r), \tag{3}$$

where δ denotes the Dirac delta function. The expression implicates that the single hammer of the tapping machine generates a spectrum with harmonics with a 2 Hz frequency step [12].

In case of a real tapping machine, some variation between the individual force pulses may be expected. If only a single force pulse $F(t)$ of the hammer is being considered, the amplitude spectrum is

$$F_n = \int_0^{T_r} F(t) e^{-i2\pi nt} dt. \tag{4}$$

The mechanical impulse I exerted by a hammer in the impact can be determined by integrating the time history $F(t)$ of a force pulse [4,5]

$$I = \int_0^{T_r} F(t) dt. \tag{5}$$

According to [4,5], the value of the impulse I ranges from mv_0 to $2mv_0$ depending on whether the impact is ideal inelastic or ideal elastic. The geometric mean value of the impulse I is $\sqrt{2}mv_0$. Further on, the low-frequency force F_{lf} can be determined dividing the impulse with the period between the pulses T_r

$$F_{lf} = \frac{I}{T_r}. \tag{6}$$

The low-frequency force F_{lf} (or the impulse I divided with the force period T_r) is equivalent with the low-frequency values of the magnitude of the amplitude spectrum $|F_n|$. Theoretically, the range of variation of the level of the F_{lf} is 6 dB [4]. This corresponds the maximum possible change in the momentum exerted by the apparatus.

The force level in [dB] can be calculated, e.g. in 1/3-octave-band frequencies, as follows

$$L_{force} = 20\log\left(\frac{F_{rms}}{F_{ref}}\right), \tag{7}$$

where F_{rms} denotes the root-mean-square force for each frequency band, and F_{ref} is the reference force.

When comparing the excitation of different floors in the frequency domain, the magnitude of the amplitude spectrum $|F_n|$ of the single force pulses (later also briefly called *the force spectrum*) is of particular interest. Additionally, the differences in the excitation force can be seen from the force level results. Moreover, the impulse I (or the low-frequency force F_{lf}) exerted by an impact represents the interaction between the hammer and the floor.

2.2. Procedure of the experiments

Impact force excitation was studied using an instrumented ISO tapping machine. The centre hammer of the machine (Norsonic Nor277) was modified and equipped with both force and acceleration sensors (see Fig. 1). The force sensor (Kistler type 9712B5000), covered with a custom-built impact cap, was placed at the bottom of the hammer in order to measure the impact force input into the floor. The acceleration sensor (Kistler type 8202A10) was placed at the top of the hammer to get further information on the motion of the hammer.

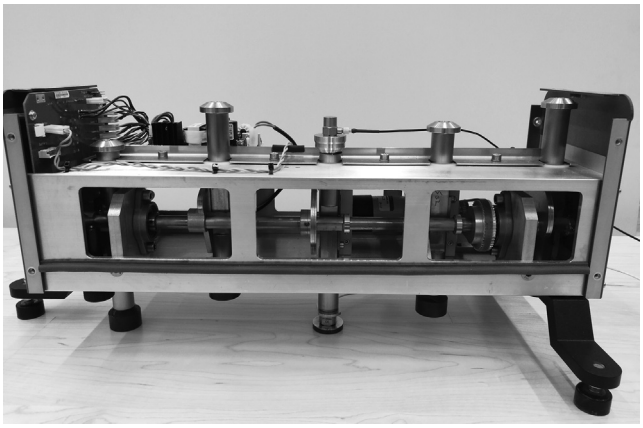

Fig. 1. The instrumented ISO tapping machine. The centre hammer was modified and equipped with force and acceleration sensors.

The hammer itself was modified to fulfil the requirements for the tapping machine presented in the standards [1,2] together with the attached sensors and additional parts. Thus, e.g. the diameter of the custom-built impact cap was 30 mm and the curvature of the impact surface of the cap was 500 mm. Additionally, the mass of the instrumented hammer was set to 503 g and the falling height of the hammer was kept at 40 mm. The permitted range of the mass of the hammer is 488–512 g [1,2], so the hammer fulfilled this requirement. The unmodified original hammer of the tapping machine weighted 502 g. Fig. 2 depicts the original hammer and the instrumented hammer used in the measurements. The sensors

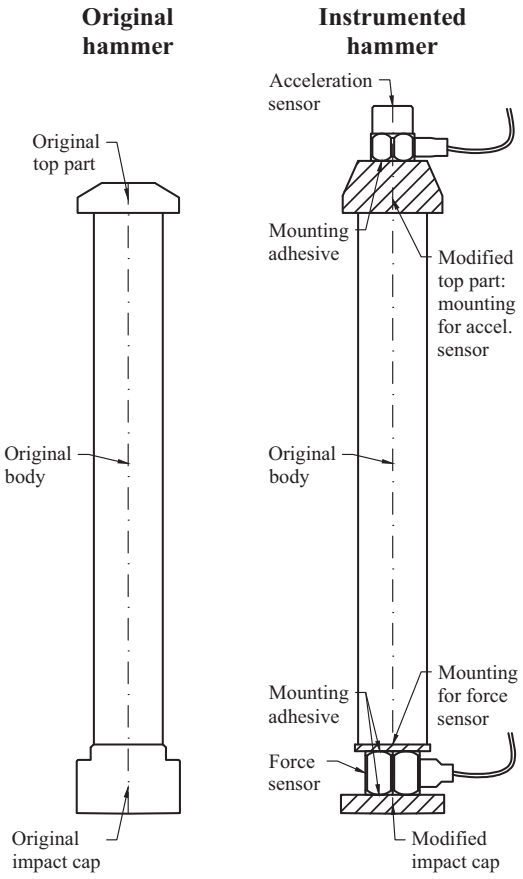

Fig. 2. The original and the instrumented hammer of the ISO tapping machine.

were mounted to the body of the hammer with studs. Moreover, adhesive was used in the mounting between the sensors and the body.

The impact force was directly measured from the hammer during the normal operation of the apparatus. This way the variation of the impact force pulses could be investigated. In the research [15], Gudmundsson noticed that the motion of the other hammers disturbed the signal when the force measurements were carried out using an acceleration sensor. Because of this, all the measurement results presented in this paper were derived from the signal of the force sensor in order to neglect the contribution of the other hammers to the impact force under study. It was assumed that the hammer behaved in these measurements as a rigid body. Therefore, the actual driving force would be the counterforce of the measurement signal during the contact of the hammer and the floor.

At the beginning of each measurement, the hammers of the tapping machine were at rest in arbitrary positions. The measurement started when the instrumented hammer first hit the surface of the floor. All measurements were performed in the time-domain, and therefore the time history of the impact force was recorded. The length of each measurement was approximately 30 s and the sampling frequency was 12800 Hz. During the experiments, the measurement cables were fastened with tape to the body of the tapping machine, in order to not interfere with the acceleration and force measurements.

2.3. Floor structures and source positions

The experiments were carried out on 24 wooden floors (see Fig. 3). The sizes of the floors were 2.4 m × 2.7 m with a span of 2.7 m. Two bearing floor structures were studied: a 100 mm thick cross-laminated-timber (CLT) slab (floors F1–F5) and a prefabricated rib slab (floors F6–F10). The CLT-slab was 3-layered with lamellas of thicknesses 30, 40, and 30 mm. The rib slab was constructed from 25 mm thick LVL panel deck and 45 mm × 260 mm LVL beams (c/c 578–600 mm). The LVL panel was both screwed and glued to the beams of the rib slab. For more information of the load bearing floors, see the Appendix 1 presented in the supplemental material. In few experiments, additional plasterboards were attached to the surface of the bearing structures in order to increase the mass of the floor. The plasterboards were glued and screwed to each other.

The surface structures of the floors included a multilayer parquet on an underlayment, a cushion vinyl, and a floating floor. The dynamic stiffness per unit area s' and the apparent dynamic stiffness per unit area s_t' [20] of the resilient products were measured. The multilayer parquet used in the measurements was a 14 mm thick maple parquet equipped with tongue-and-groove joints. In all the measurements, the parquet was installed in identical order on the soft 3 mm thick underlayment. The cushion vinyl was a soft 3 mm thick product especially used in apartment houses. The vinyl was glued to the substructure under and around each source position. The floating floor was constructed from a 30 mm thick mineral wool layer and two plasterboard layers glued and screwed to each other according to manufacturer's instructions. Since the floating floor was constructed from individual plasterboard sheets, there were small gaps between adjacent boards. One gap between the lower layer of the plasterboards lied in the centre of the span.

The load bearing structures were installed between vibration isolated massive steel structures placed on the floor of the construction laboratory. The structures were fixed from their both ends to the load supports with screw connections (see supplemental material, Appendix 2). The natural frequency of the vibration isolation was set under 10 Hz in order to attenuate possible vibrations from the surroundings. The frequency range of interest was

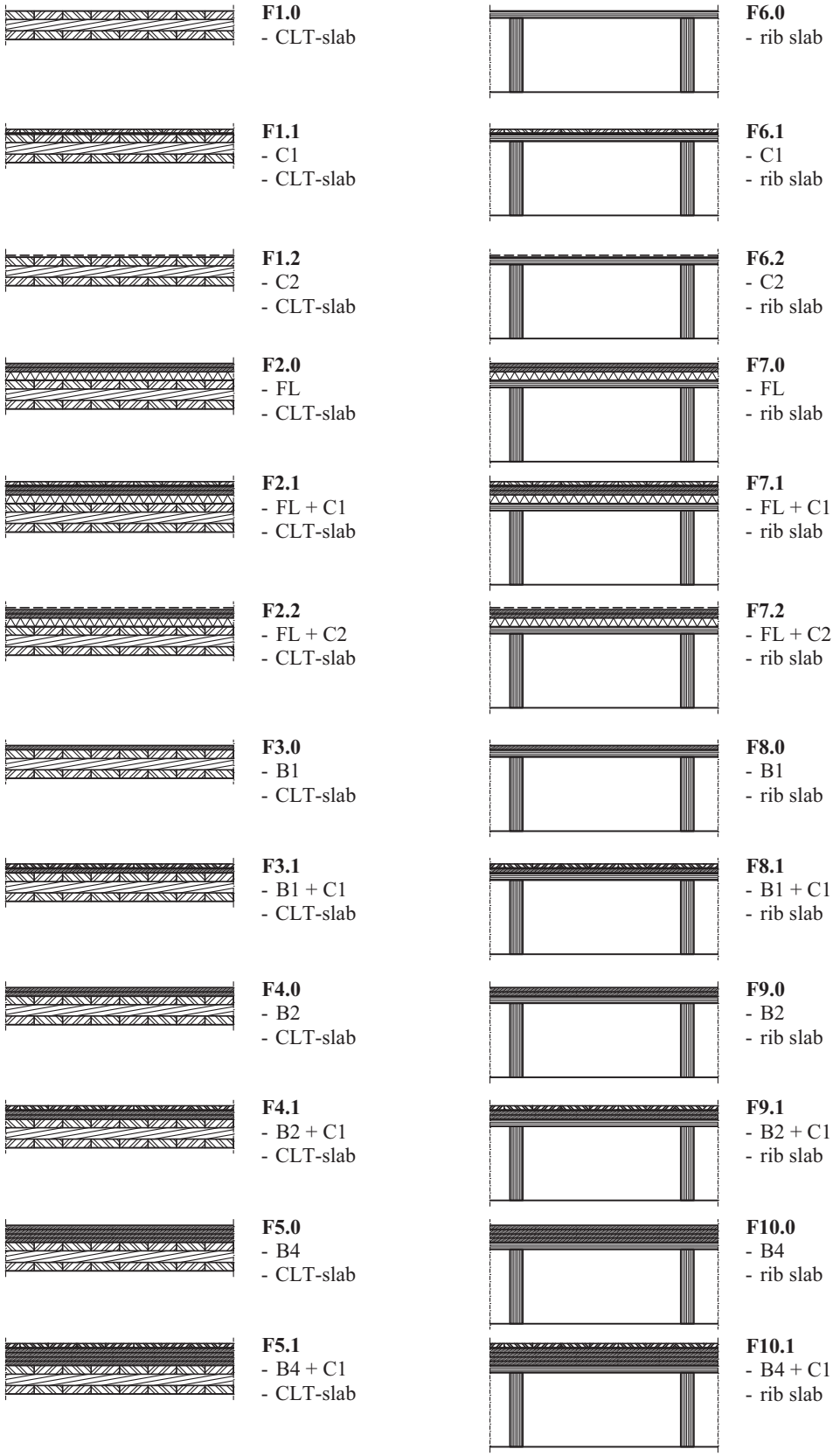

Fig. 3. Floor structures F1–F10. The number after the point indicates the type of the floor covering on the floor as follows: (0) no floor covering; (1) C1, the multilayer parquet (thickness h = 14 mm) on an underlayment (h = 3 mm, s' = 65,1 MN/m^3); and (2) C2, the cushion vinyl (h = 3 mm, s' = 2282 MN/m^3). The other abbreviations are: FL, a floating floor with two plasterboards (h = 15 mm, mass per unit area m' = 15.4 kg/m^2) on a mineral wool layer (h = 30 mm, s'_t = 12,8 MN/m^3, s' = 16,4 MN/m^3); and B, additional plasterboards ((h = 15 mm, m' = 15.4 kg/m^2) on the bearing structure, where the number following B denotes the number of the plasterboards layers (B1, B2, B4).

16–3600 Hz, since the low frequency behaviour often determines the subjective rating of the wooden floor structures, cf. [21,22].

The measurements were performed at five source positions S1–S5 per structure. Fig. 4 shows the source positions and the orientation of the ISO tapping machine at the positions. The positions were at least at a range of 0.5 m from the edges of the structure (cf. requirements in ISO 16283-2 [2]). The position S3 was located at the centre of the structures. All the positions were kept the same for all studied floor structures.

2.4. Post-processing of the measurement results

Fig. 5**a** shows an example of the entire measured time history of the force. As the impact force generated by the ISO tapping machine was measured with the sensor attached to the hammer, a slight additional force occurred between the impacts upon the floor (see Fig. 5**b**). This was due to the acceleration of the instrumented hammer and due to the impacts generated by the hammers not involved in the measurement. However, the counterforce of the force being measured drives the floor only when the hammer and the surface of the floor are in contact. Thus, in order to get information from the actual driving force of the floors, all the impact force pulses were sought, and the force was set to zero between the impacts.

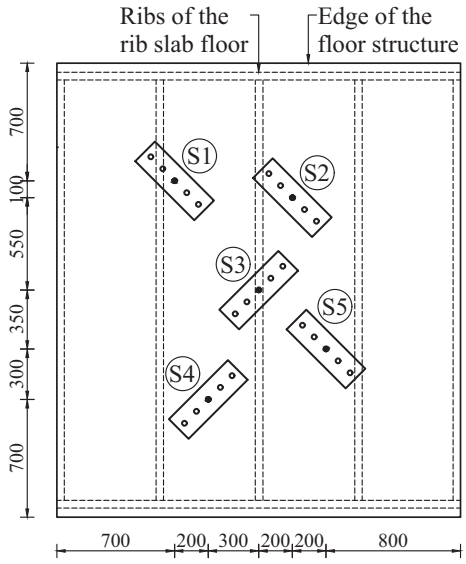

Fig. 4. Source positions S1–S5 on the floor structure. The rectangular boxes illustrate the orientation of the ISO tapping machine on the source positions and the black circles show the location of the instrumented hammer used in the measurements. Dimensions in the figure are presented in millimetres.

Since the position of the hammer in the beginning of each measurement was arbitrary, not resulting in a full initial impact, the first impact was omitted from the time history of the force. In addition, the time history from the beginning of the last impact to the end of the measurement was deleted, because of the lack of information of the beginning of the next impact after the measurement (the time between the impacts was not exactly 0.5 s, which can also be seen from Fig. 5**b**).

The spectrum of the driving force was determined from the time history of the force processed in accordance with the method described above. The amplitude spectrum F_n of the driving force was determined for every force pulse according to Eq. (4). The calculations were carried out with the FFT algorithm implemented in MATLAB®. In order to compare different force pulses in the frequency domain, the length of the period between the pulses T_r was set to 500 ms. The amount of the samples in a single force period was 6400, thus resulting in frequency spacing of the spectrum of 2 Hz.

Additionally, the time history of the force was filtered using 1/3-octave-band filters in the frequency range from 20 to 3150 Hz. The root-mean-square force F_{rms} was calculated for each frequency band and the force level L_{force} was determined by using Eq. (7).

In order to determine the effect of the floor on the momentum exerted by the hammer, the mechanical impulse I was determined according to Eq. (5) for every force pulse. The calculations of the integral were performed via the trapezoidal method implemented in MATLAB®. Hence, the results for I represent the approximate values of the impulse.

The calculations were done for every floor under study and for every source position S1–S5. Note that the values of the calculated force spectra were low compared to the measured peak values of the impact force pulses in time domain. This occurred, since between the short impacts upon the floor, the force driving the floor was zero, and the calculation of the force spectra was carried

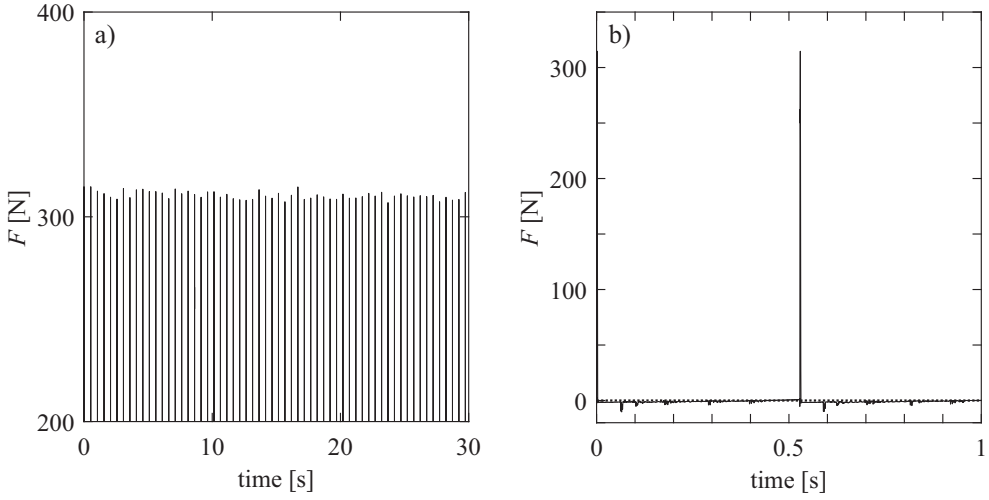

Fig. 5. Time history of the force (floor F1.1, source position S1): a) an example of the entire time history; b) an example of the additional force occurring between the first two impacts of the instrumented hammer (the black solid line depicts the measurement result and the dotted line the force level of zero Newtons).

out also for these moments (see Eq. (4)). If the results were compared with the one-sided formulation of the Fourier series, the values of the magnitude of the amplitude spectra and the impulses should be multiplied with the factor of 2.

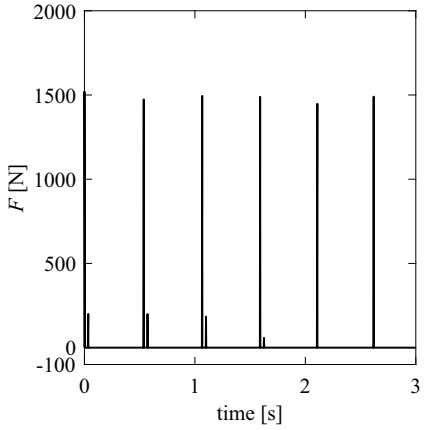

Fig. 6. The secondary impacts of the hammer during the force measurement (floor F7.0, source position S5). The second impacts occurred 34 ms after each of the first four impacts on this floor. These first impacts were omitted from the calculation of the results. No secondary impacts occurred on the other floors under study.

2.5. The secondary impacts of the hammer

In theory, it is possible that the hammer of the ISO tapping machine would rebound and hit the floor at least a second time. These secondary impacts could occur when the first impact is nearly inelastic and almost all the energy is dissipated in the collision. The standards ISO 10140-5 and ISO 16283-2 have set a requirement that the time between the impact and the lift of the hammer should be less than 80 ms [1,2]. This sets the possible time window for the secondary impacts. Wittstock showed a measurement result in [12] where the hammer of the mechanical tapping machine began to fall again after the actual impact and before its lift. His experiments were performed on a small reception plate made of artificial stone. However, in this occasion the hammer did not hit the plate a second time.

In this study, it was also investigated whether the measurement results included secondary impacts. This was carried out by comparing the modified force signal (see Section 2.4) with the original force signal between the actual impacts. According to the results, second impacts occurred approximately 34 ms after the first four full impacts on the floor F7.0 at the source position S5 (see Fig. 6). These first impacts were omitted from the calculations and no spectra for these impacts were determined. This was the only occasion where the second impacts were prominent and no

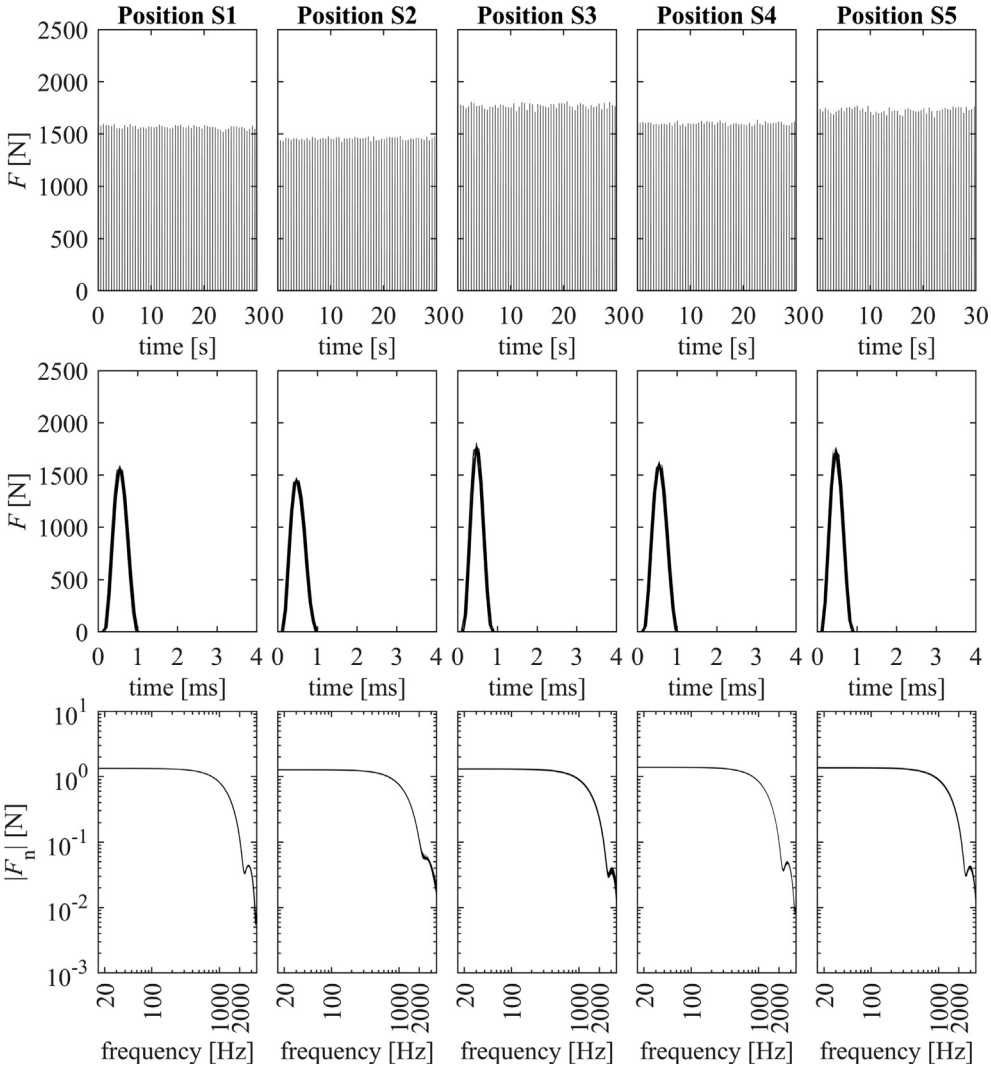

Fig. 7. An example of the measurement results (floor F1.0). Results for source positions S1–S5 are shown in three rows. The top row shows the time history of the force driving the floor, the individual force pulses are presented in the middle row and the bottom row depicts the magnitude of the amplitude spectra $|F_n|$.

secondary impacts occurred on the other floors under study. Hence, it is justified to carry out the calculation of the force spectrum on basis of the post-processing method described in the previous Section 2.4.

3. Results

3.1. The impact force in time and frequency domains

All the measurement results of the impact force have been shown in the Appendix 3 of the supplemental material. An example of the presentation of the results is illustrated in Fig. 7. The results in the appendix were arranged on three rows as follows: the top row shows the time history of the force driving the floor for the whole measurement period, the second row presents the individual force pulses in time domain, and the magnitudes of the amplitude spectra $|F_n|$ of the single force periods is depicted on the bottom row. The five columns of the figure represent results for each source position S1–S5. The individual force pulses were centred based on their peak values in order to make them better comparable. In a few cases, the pulse had two local maxima, when the pulses were primarily centred based on the first one. The amount of impacts ranged from 60 to 61 during the measurements (without the first and the last impact).

In Fig. 7 the variation of the impacts on different source positions can be seen both from the time histories and from the spectra of the forces. However, since the measured values were discrete, the variation of the excitation force was best evident in the individual force pulses, where the shape of the pulses was prominent. The results for the spectra of the force presented for a single source position form a set of curves, for the calculations were carried out for every individual force period. Thus, these results also indicate the variation of the excitation in the frequency domain.

The force spectra presented in the results were derived by assuming that the hammer would behave as a rigid body. However, if the joints between the parts of the instrumented hammer and the force sensor would behave elastically, this would affect the behaviour of the hammer. Hence, it should be noted that in some cases and in the whole frequency range presented, the spectra may not correspond to the impacting force correctly.

The dependence of the force pulses in the time domain on the floor and source position can also be seen from Table 1, where the peak values of the individual force pulses and their durations have been listed. The durations of the pulses represent the length

Table 1
The average peak values and the average durations of the individual force pulses.

Floor		Pos. S1	Pos. S2	Pos. S3	Pos. S4	Pos. S5
F1.0	Peak value [N]	1566.6	1457.1	1770.2	1601.4	1727.2
	Duration [ms]	0.99	1.02	0.91	1.01	0.94
F1.1	Peak value [N]	310.5	345.1	421.1	439.9	397.4
	Duration [ms]	3.02	2.44	2.41	2.20	2.38
F1.2	Peak value [N]	624.0	647.1	661.9	627.8	623.4
	Duration [ms]	2.10	2.15	2.00	2.16	2.24
F2.0	Peak value [N]	1149.8	1523.0	1008.5	1474.7	1564.0
	Duration [ms]	1.08	0.94	1.26	0.94	0.95
F2.1	Peak value [N]	287.4	338.2	410.8	445.5	400.2
	Duration [ms]	3.26	2.56	2.44	2.10	2.35
F2.2	Peak value [N]	540.2	556.6	547.5	580.6	559.8
	Duration [ms]	2.43	2.36	2.45	2.32	2.45
F3.0	Peak value [N]	1471.2	1831.4	1918.8	1764.3	1712.5
	Duration [ms]	0.98	0.82	0.85	0.87	0.88
F3.1	Peak value [N]	341.5	359.4	419.8	462.1	412.5
	Duration [ms]	2.83	2.46	2.36	2.15	2.33
F4.0	Peak value [N]	1604.3	1967.3	1792.3	1704.1	1524.1
	Duration [ms]	0.87	0.81	0.86	0.85	0.95
F4.1	Peak value [N]	324.0	351.5	422.5	420.9	407.2
	Duration [ms]	2.92	2.50	2.33	2.28	2.37
F5.0	Peak value [N]	1885.9	1820.5	2150.6	2178.3	1693.1
	Duration [ms]	0.83	0.86	0.77	0.78	0.88
F5.1	Peak value [N]	345.3	374.3	423.8	417.2	423.8
	Duration [ms]	2.90	2.49	2.36	2.26	2.30
F6.0	Peak value [N]	673.1	613.0	1252.0	575.1	577.9
	Duration [ms]	1.91	1.82	1.24	2.10	2.49
F6.1	Peak value [N]	358.9	412.7	440.9	508.9	420.6
	Duration [ms]	2.83	2.58	2.35	1.94	2.68
F6.2	Peak value [N]	502.6	458.0	567.2	444.3	425.7
	Duration [ms]	2.35	3.02	2.19	2.42	3.21
F7.0	Peak value [N]	1502.7	1470.7	1127.2	1566.4	1501.0
	Duration [ms]	0.89	1.04	1.07	0.90	0.92
F7.1	Peak value [N]	321.7	366.0	407.0	481.2	435.8
	Duration [ms]	3.04	2.59	2.52	2.14	2.24
F7.2	Peak value [N]	544.7	539.3	523.4	529.6	546.9
	Duration [ms]	3.02	2.70	2.74	2.90	2.58
F8.0	Peak value [N]	1124.4	1255.7	1435.5	1192.0	1170.3
	Duration [ms]	1.20	1.13	0.96	1.14	1.13
F8.1	Peak value [N]	361.1	396.4	470.5	477.4	436.8
	Duration [ms]	2.96	2.56	2.48	2.14	2.59
F9.0	Peak value [N]	992.0	1917.5	1728.8	1476.0	1833.9
	Duration [ms]	1.20	0.79	0.85	0.93	0.81
F9.1	Peak value [N]	336.8	352.9	425.3	469.8	388.2
	Duration [ms]	2.90	2.51	2.46	2.05	2.36
F10.0	Peak value [N]	1820.2	2045.7	1180.0	1387.6	1358.2
	Duration [ms]	0.84	0.80	1.15	1.02	1.01
F10.1	Peak value [N]	316.2	362.6	419.7	455.9	393.1
	Duration [ms]	2.96	2.39	2.47	2.13	2.33

of the pulse from the beginning to the end of it. The values presented in the table correspond to the averaged results for the respective floor and source position.

3.2. The average impact force in the frequency domain

Fig. 8 shows the average of all the magnitudes of the amplitude spectra $|F_n|$ of the individual force periods for each floor in the frequency range 16 to 3600 Hz. The figure illustrates the results for the source position S1. The spectra depicted in the figure represent the arithmetic averages of the spectra of all the individual force periods of the respective floor. The figure includes a small window for magnified results in the low frequencies from 16 to 200 Hz, where the variation of the results in this frequency range can be seen.

Fig. 9 shows the force levels L_{force} in 1/3-octave-bands from 20 to 3150 Hz for each floor structure. The results are arithmetic averages over all the source positions S1–S5. In the Fig. 10, the standard deviations of these levels over the source positions are shown. Thus, the figure depicts the effect of the source position on the force measured on each floor.

In the Figs. 8–10, the results for the floors without any floor covering (floor types Fx.0) are presented with solid lines, the dashed lines show the results for the floors with the multilayer parquet on the underlayment (floor types Fx.1), and the results for the floors with the cushion vinyl as the floor covering (floor types Fx.2) are depicted with dash-dotted lines.

3.3. The mechanical impulses generated by the ISO tapping machine

Table 2 shows the average impulses I and their standard deviations calculated for all the floors at the source positions S1–S5. Additionally, the average values are depicted in Fig. 11, where the scale is set such that the extreme boundaries represent the theoretical limits for the ideal inelastic and ideal elastic impulse discussed in the Section 2.1. The geometrical mean value of the impulse ($\sqrt{2}mv_0 \approx 0.626$ Ns) is illustrated in Fig. 11 with dotted line. If the low-frequency force F_{lf} were determined on the basis of the impulses (see Eq. (6)), they would correspond the low-frequency values of the magnitude spectra presented in Fig. 8.

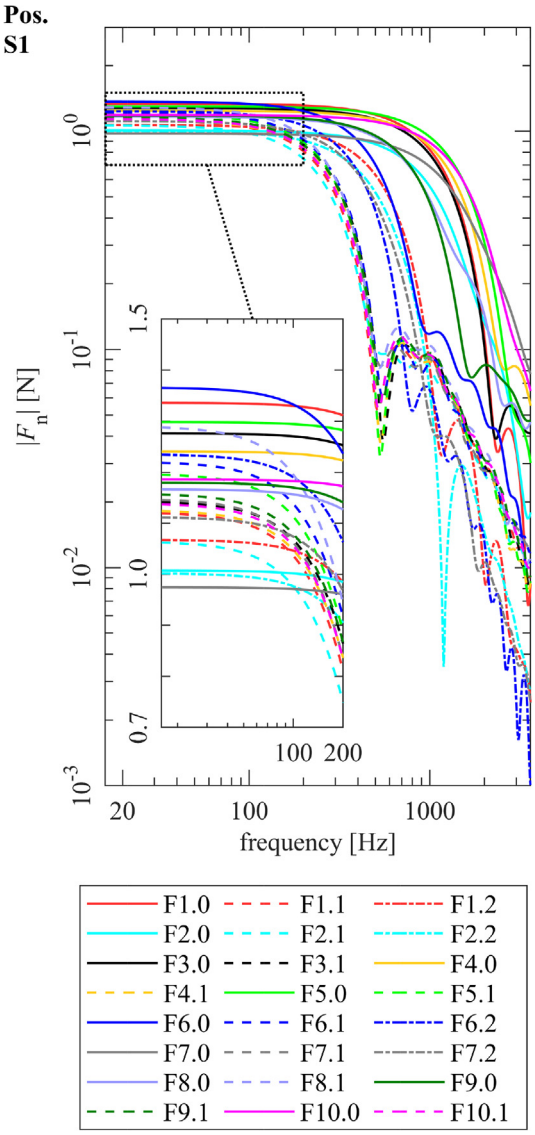

Fig. 8. The average of the magnitudes of the amplitude spectra $|F_n|$ of the force on all the floors at the source position S1. The solid lines depict the result on a floor without any floor covering, the dashed lines present the result when the floor covering was the multilayer parquet on the underlayment, and the dash-dotted lines illustrate the results on the cushion vinyl.

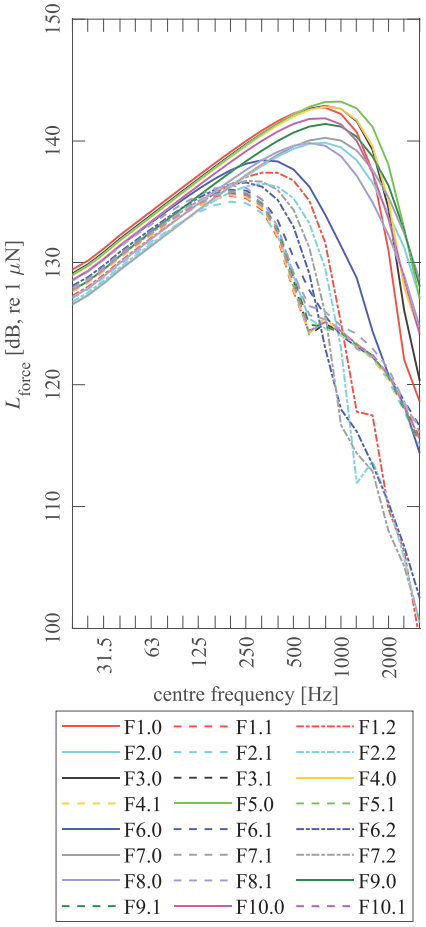

Fig. 9. The average force level L_{force} over all the source positions S1–S5 in 1/3-octave-bands on all the floors. The solid lines depict the result on a floor without any floor covering, the dashed lines present the result when the floor covering was the multilayer parquet on the underlayment, and the dash-dotted lines illustrate the results on the cushion vinyl.

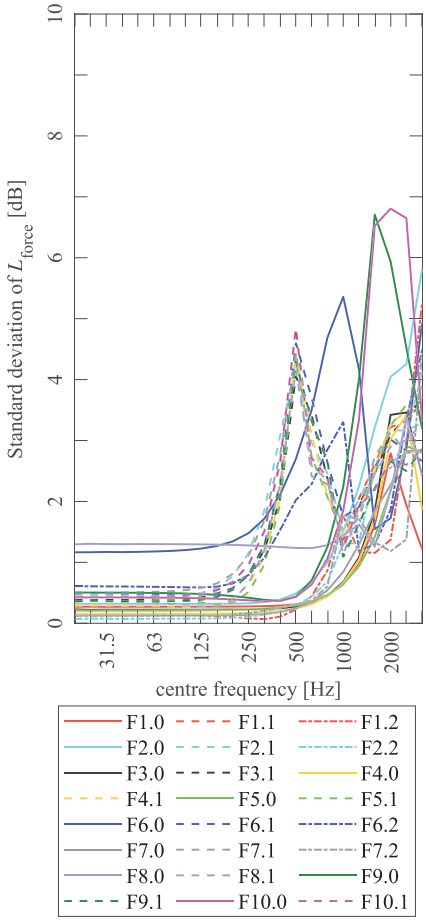

Fig. 10. The standard deviation of the force level L_{force} over the source positions S1–S5 in 1/3-octave-bands on all the floors. The solid lines depict the result on a floor without any floor covering, the dashed lines present the result when the floor covering was the multilayer parquet on the underlayment, and the dash-dotted lines illustrate the results on the cushion vinyl.

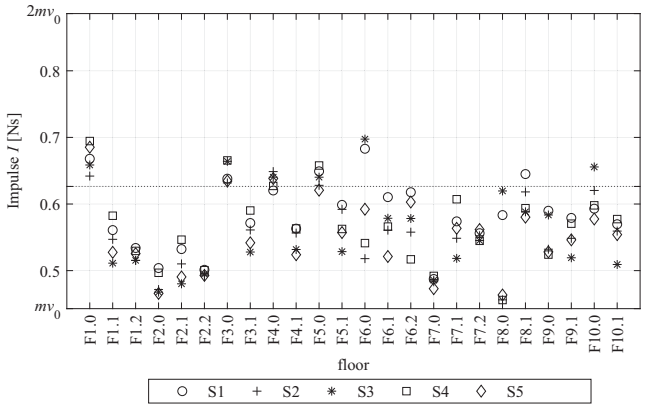

Fig. 11. The average impulses I on different floors at the positions S1–S5. The extreme boundaries represent the theoretical limits for the impulse from 0.443 Ns (mv_0) to 0.886 Ns ($2mv_0$) which correspond to the ideal inelastic and ideal elastic collisions, respectively. The theoretical geometrical mean value of the impulse 0.626 Ns ($\sqrt{2}mv_0$) is illustrated with the dotted line.

4. Discussion

4.1. The impact force excitation on different wooden floors

The results for the peak values of the force pulses caused by the tapping machine and their durations (Table 1), and for the force spectra (Fig. 8), as well as for the force level spectra (Fig. 9), indicate that the excitation driving the wooden floors depends strongly on the type of the structure. The finding is of very high practical importance. Such a wide experimental evidence has not been published previously in this field. When comparing the results for the force spectra with the spectra measured on concrete and steel structures in [11,15,17], it is obvious that the impact force excitation generated by the ISO tapping machine is different on the wooden floors. The variation of the results for the force spectra on different wooden floors is evident in the whole frequency range of interest, but the differences are major above 500 Hz. At frequen-

Table 2
The average values and the standard deviations of the impulses I in [Ns] determined from all the individual force pulses. The standard deviations are presented in brackets. The average values (AVG) and standard deviations (STDEV) of the results are shown for each floor (on the right part of the table).

Floor	Pos. S1	Pos. S2	Pos. S3	Pos. S4	Pos. S5	AVG	STDEV
F1.0	0.67 (0.0031)	0.64 (0.0031)	0.66 (0.0050)	0.69 (0.0037)	0.69 (0.0051)	0.67	0.0192
F1.1	0.56 (0.0033)	0.55 (0.0028)	0.51 (0.0030)	0.58 (0.0031)	0.53 (0.0032)	0.55	0.0251
F1.2	0.53 (0.0021)	0.52 (0.0017)	0.52 (0.0021)	0.53 (0.0026)	0.53 (0.0026)	0.52	0.0079
F2.0	0.50 (0.0019)	0.47 (0.0020)	0.47 (0.0017)	0.50 (0.0024)	0.47 (0.0013)	0.48	0.0161
F2.1	0.53 (0.0028)	0.51 (0.0021)	0.48 (0.0019)	0.55 (0.0034)	0.49 (0.0018)	0.51	0.0250
F2.2	0.50 (0.0013)	0.49 (0.0018)	0.49 (0.0018)	0.50 (0.0018)	0.49 (0.0013)	0.50	0.0041
F3.0	0.64 (0.0030)	0.63 (0.0031)	0.66 (0.0036)	0.67 (0.0037)	0.63 (0.0028)	0.65	0.0152
F3.1	0.57 (0.0036)	0.56 (0.0021)	0.53 (0.0024)	0.59 (0.0032)	0.54 (0.0029)	0.56	0.0221
F4.0	0.62 (0.0024)	0.65 (0.0034)	0.64 (0.0038)	0.63 (0.0024)	0.64 (0.0023)	0.63	0.0104
F4.1	0.56 (0.0050)	0.56 (0.0023)	0.53 (0.0025)	0.56 (0.0028)	0.52 (0.0023)	0.55	0.0169
F5.0	0.65 (0.0026)	0.63 (0.0036)	0.64 (0.0039)	0.66 (0.0033)	0.62 (0.0031)	0.64	0.0139
F5.1	0.60 (0.0044)	0.59 (0.0033)	0.53 (0.0034)	0.56 (0.0029)	0.56 (0.0031)	0.57	0.0256
F6.0	0.68 (0.0058)	0.52 (0.0063)	0.70 (0.0056)	0.54 (0.0052)	0.59 (0.0062)	0.61	0.0730
F6.1	0.61 (0.0078)	0.56 (0.0053)	0.58 (0.0056)	0.57 (0.0037)	0.52 (0.0048)	0.57	0.0295
F6.2	0.62 (0.0040)	0.56 (0.0051)	0.58 (0.0024)	0.52 (0.0048)	0.60 (0.0053)	0.57	0.0358
F7.0	0.49 (0.0013)	0.48 (0.0014)	0.49 (0.0013)	0.49 (0.0014)	0.47 (0.0015)	0.48	0.0065
F7.1	0.57 (0.0094)	0.55 (0.0073)	0.52 (0.0058)	0.61 (0.0059)	0.56 (0.0071)	0.56	0.0301
F7.2	0.56 (0.0019)	0.55 (0.0031)	0.55 (0.0031)	0.54 (0.0029)	0.56 (0.0020)	0.55	0.0070
F8.0	0.58 (0.0023)	0.46 (0.0021)	0.62 (0.0021)	0.46 (0.0016)	0.46 (0.0023)	0.52	0.0712
F8.1	0.65 (0.0077)	0.62 (0.0035)	0.59 (0.0042)	0.59 (0.0061)	0.58 (0.0054)	0.61	0.0243
F9.0	0.59 (0.0023)	0.53 (0.0026)	0.58 (0.0025)	0.52 (0.0021)	0.53 (0.0023)	0.55	0.0291
F9.1	0.58 (0.0022)	0.55 (0.0018)	0.52 (0.0018)	0.57 (0.0024)	0.55 (0.0022)	0.55	0.0211
F10.0	0.59 (0.0035)	0.62 (0.0024)	0.66 (0.0028)	0.60 (0.0019)	0.58 (0.0022)	0.61	0.0273
F10.1	0.57 (0.0020)	0.56 (0.0035)	0.51 (0.0018)	0.58 (0.0017)	0.55 (0.0017)	0.55	0.0239

cies below 100 Hz, the values of the force spectra stay rather constant and the differences between the floors were minor in comparison with the high-frequency range results. However, the value of the magnitude force spectra ranged from 0.9 to 1.4 N. This variation corresponds to the level difference of over 3 dB of the force input in the low-frequency range (see Fig. 9).

The variation of the results in the low-frequency range can also be seen from the impulses I shown in Table 2 and Fig. 11, as discussed in Section 2.1. On the basis of these results, the geometrical mean value of the impulse does not represent the actual value of the impulse on wooden floors in general. The results imply that the model describing the impact force excitation generated by the ISO tapping machine on wooden floors should include the ability to predict the value of the impulse. This is especially important when developing mathematical calculation tools predicting the impact sound insulation of wooden floors in the low-frequency range.

In case of the CLT-floors (F1.0, F3.0, F4.0 and F5.0), the impulses and the force spectra had on average the greatest values of all the results. The shapes of the force spectra on different CLT-floors were rather uniform and they began to decrease around 500 Hz, while the first local minima occurred at over 2000 Hz. On the bare CLT-floor (F1.0), the force was between 1.28 and 1.39 N in the low-frequency range. The respective values ranged from 1.24 to 1.33 N on the CLT-floors with additional plasterboards (F3.0, F4.0 and F5.0). Correspondingly, the impulses were 0.64–0.69 Ns and 0.62–0.67 Ns on the floor F1.0 and on the floors F3.0, F4.0 and F5.0, respectively. Thus, the impulses were a little above the geometrical mean value and the differences between the results at different source positions were minor. The results imply that in case of massive wooden plates the impact force excitation generated by the ISO tapping machine is quite independent on the position of the apparatus.

In case of the rib slab floors (F6.0, F8.0, F9.0 and F10.0), the effect of the thin wooden deck and the ribs on the force was prominent. When the source position was above the rib or in the vicinity of it (at S1 or S3), the force spectra had higher values than at the other source positions. This occurred especially on the floors F6.0 and F8.0, but the differences diminished when the floor included at least two layers of plasterboards (floors F9.0 and F10.0). On the floor F6.0, the shape of the spectra measured at the source positions between the ribs (S2, S4 and S5) resembled the spectra measured on the floors equipped with the floor coverings. In the low-frequency range the force spectra had values 1.04–1.39 N on the floor F6.0, and values 0.9–1.31 N on the floors F8.0, F9.0 and F10.0. Respectively, the impulses exerted by the hammer ranged from 0.52 to 0.70 Ns and between 0.46 and 0.66 Ns, on these floors. These variations correspond to the force level difference of even 3 dB of the force input in the low-frequency range. This kind of behaviour was prominent also in the results presented by Gudmundsson [15], where the measured force level spectrum was lower even in the low-frequency range when the floating floor was a lightweight structure in comparison with concrete floating floors. Therefore, it seems justified to recommend more impact source positions in addition to the minimum number of positions when measuring the impact sound insulation of rib slab floors, cf. [2]

When the surface structure was the bare floating floor (floors F2.0 and F7.0), the results were rather uniform and independent of the source position. The force spectra ranged from 0.93 to 1.01 N in the low-frequencies and started to decrease around 500 Hz. In correspondence with the low-frequency results, the impulses varied from 0.47 to 0.50 Ns. Therefore, the impact of the hammer upon these floors could be regarded as nearly inelastic. This is one reason why the secondary impacts occurred on the floor F7.0, as discussed in Section 2.5. The minor differences between the results for the floors F2.0 and F7.0 imply that the bearing structures below the floating floors did not affect the force generation on the floating floors differently.

When the floor coverings were installed on the CLT-floors, the low-frequency values of the force spectra and the impulses decreased. This phenomenon did not occur on all the rib slab floors. Interestingly however, installing the floor coverings on the floating floor structures increased these values.

When the floor covering was the multilayer parquet with the underlayment (floor types Fx.1), the shapes of the force spectra were similar on the respective source positions. The force spectra began to decrease around 100 Hz and reached their first local minima in the frequency range from 500 to 800 Hz depending on the source position. In the low-frequency range, the force spectra had values 0.96–1.29 N. Correspondingly, the impulses were between 0.48 Ns (nearly inelastic impact) and 0.64 Ns (near the geometrical mean value of the impulse). However, the differences between the results on the same floor corresponded to the level difference of at most 1.3 dB of the force input in the low-frequency range. The differences between the different source positions presumably originated from the different distances between the respective source position and the tongue-and-groove joint of the parquet. The resemblance of the results at the corresponding source positions was also prominent in the individual force pulses (see Appendix 3 of the supplementary material). The force pulses had often two local maxima, which probably occurred due to the behaviour of the surface structure under the hammer. When the hammer first hit the floor, the first local peak occurred. After this moment, the parquet shortly bended and during this the hammer and the floor were in contact. When the bending stopped, the second local maximum followed. The results imply that the structure under the multilayer parquet with the underlayment has little effect on the force input of this floor type, but the local behaviour of the parquet determines the driving force of the floor.

When the cushion vinyl was the floor covering (floor types Fx.2), the behaviour of the force spectra was similar to that of the floor types Fx.1 discussed above. The force spectra began to decrease around 100 Hz as with the parquet. However, the first local minima occurred at higher frequencies than on the floors Fx.1, at above 800 Hz. In the low-frequency range the force spectra had values between 0.98 and 1.23 N. Respectively, the impulses ranged from 0.49 Ns (nearly inelastic impact) to 0.62 Ns (near the geometrical mean value of the impulse). When the substructure under the cushion vinyl was the CLT-slab (floor F1.2) or the floating floor (floors F2.2 and F7.2), the differences between the impulses on different source positions were minor, and less than with the floor types Fx.1. In case of the floor F6.2, where the load bearing floor was the rib slab, the differences between the spectra and the impulses on different source positions were greater because of the different distance between the source positions and the ribs.

4.2. The time dependency of the impact force

The standards [1,2] state that the impact sound pressure levels can reveal time dependency after the tapping is started. Hence, the time dependency of the impact force excitation was also studied. According to the measurement results the impact force did not seem to vary over time. This is evident from the results of the individual force pulses presented in the Appendix 3 of the supplemental material (see also Fig. 7) and from the standard deviations of the force impulses (Table 2). This suggests that in case of the measured wooden floors the overall spectrum of the force excitation can be determined based on the first few impacts upon the floor after rather steady impacting conditions have been achieved. This

implies that the process of excitation of the wooden floors was not transient. Thus, the vibration of the measured wooden floors did not significantly affect the excitation force generated by the ISO tapping machine and a transient force model, such as presented in [11], might not be necessary to describe the impact force excitation on wooden floors.

5. Conclusions

This paper presented a procedure for measuring the impact force excitation generated by the ISO tapping machine and showed measurement results on 24 wooden floors. Such a wide experimental evidence has not been published previously in this field. The experiments were carried out with an instrumented ISO tapping machine, which measured the force generated in the impacts of the hammer upon the floor. With the described post-processing method, the impact force excitation driving the floor was determined. The measurement results were shown for the magnitude of the amplitude spectrum of the force and for the impulse generated in the collision of the hammer and the floor. Additionally, the average peak values and the duration of the force pulses were presented.

The differences between the force spectra on different wooden floors were prominent especially at frequencies above 500 Hz. Comparing the results with the spectra measured on concrete and steel structures shown in the literature revealed essential differences between the impact force excitation of wooden and concrete floors. At the frequencies below 100 Hz, the variation of the results was minor in comparison with the high frequencies. However, the variation in the low-frequency range corresponds to the level difference of over 3 dB of the force input. It was also noticed that the geometrical mean value of the impulse does not represent the actual value of the impulse exerted by the hammers on wooden floors.

The results for the force spectra and the impulses implied that the force driving the bare CLT-floors was rather independent on the position of the apparatus. However, in case of the rib slab floors, differences between the source positions were evident. This occurred due to the different distances between the source positions and the ribs. Adding plasterboards on the structure seemed to reduce the difference of the results between the source positions.

The force input on the bare floating floors and on the multilayer parquet with the underlayment was little influenced by the structure under these surface structures. This suggests that mostly the information of the floating structure and its material parameters are needed in order to evaluate the impact force excitation of these structures. Moreover, it was discovered that results on the floating floor did not depend on the source position. When the floor covering was the parquet, it was presumed that the differences between the source positions were caused by the different distances between the respective source position and the closest tongue-and-groove joint of the parquet.

When the floor covering was the cushion vinyl, the results were dependent on the source position only when the bearing structure was the rib slab. When the source position was between the ribs, the thin wooden deck behaved flexibly under the hammer, thus producing a lower force spectrum than at the position placed on the rib. On the other floors, the differences between the results of the source positions were minor.

According to the standards [1,2], the impact sound pressure levels can reveal time dependency after the tapping is started. The results of this paper showed that the process of excitation with the ISO tapping machine was not transient for the structures studied. Thus, no time dependency was detected, and the vibration of the measured wooden floors did not seem to influence the excitation force. This implies that a transient force model, such as presented in [11], might not be needed to describe the impact force excitation on wooden floors.

Declaration of Competing Interest

The authors declare that they have no known competing financial interests or personal relationships that could have appeared to influence the work reported in this paper.

Acknowledgements

The authors would like to thank Dr. Valtteri Hongisto and Mr. Ville Kovalainen for their constructive comments during the preparation of this manuscript. In addition, the authors would like to acknowledge Christian Berner Oy, Saint-Gobain Finland Oy, Stora Enso Oy and Upofloor Oy for donation of construction materials for this project.

Appendix A. Supplementary material

Supplementary data to this article can be found online at https://doi.org/10.1016/j.apacoust.2020.107821.

References

[1] ISO 10140–5. Acoustics – Laboratory measurement of sound insulation of building elements – Part 5: Requirements for test facilities and equipment. Geneva: International Organization for Standardization; 2010.
[2] ISO 16283–2. Acoustics – Field measurement of sound insulation in buildings and of building elements – Part 2: Impact sound insulation. Geneva: International Organization for Standardization; 2015.
[3] Rasmussen B, Machimbarrena M. Building acoustics throughout Europe—Volume 1: towards a common framework in building acoustics throughout Europe, COST Action TU0901, Brussels, 2014.
[4] Brunskog J, Hammer P. The interaction between the ISO tapping machine and lightweight floors. Acta Acust United with Acust 2003;89:296–308. , https://www.ingentaconnect.com/contentone/dav/aaua/2003/00000089/00000002/art00013.
[5] Cremer L, Heckl M, Petersson BAT. Structure-borne sound. 3rd ed. Berlin Heidelberg: Springer-Verlag; 2005.
[6] Heckl M, Rathe EJ. Relationship between the transmission loss and the impact-noise isolation of floor structures. J Acoust Soc Am 1963;35:1825–30. https://doi.org/10.1121/1.1918830.
[7] Cremer L, Heckl M, Ungar EE. Structure-borne sound. Berlin Heidelberg: Springer-Verlag; 1973.
[8] Vér IL. Impact noise isolation of composite floors. J Acoust Soc Am 1971;50:1043–50. https://doi.org/10.1121/1.1912726.
[9] Scholl W, Maysenhölder W. Impact sound insulation of timber floors: interaction between source, floor coverings and load bearing floor. Build Acoust 1999;6:43–61. https://doi.org/10.1260/1351010991501266.
[10] Lindblad S. Impact sound characteristics of resilient floor coverings. Lund Institute of Technology, Division of Building Technology, Bulletin 2, Lund, Sweden, 1968.
[11] Rabold A, Buchschmid M, Düster A, Müller G, Rank E. Modelling the excitation force of a standard tapping machine on lightweight floor structures. Build Acoust 2010;17:175–97. https://doi.org/10.1260/1351-010X.17.3.175.
[12] Wittstock V. On the spectral shape of the sound generated by standard tapping machines. Acta Acust United with Acust 2012;98:301–8. https://doi.org/10.3813/AAA.918513.
[13] Amiryarahmadi N, Kropp W, Bard D, Larsson K. Time-domain model of a tapping machine. In: Proc. Forum Acusticum 2011, Aalborg, Denmark, 2011, p. 1713–18.
[14] Coguenanff C, Guigou-Carter C, Jean P, Desceliers C. Probabilistic model of the impact force spectrum for the standard ISO tapping machine. In: Proc. 22nd Int. Congr. Sound Vib. ICSV 2015, Florence, Italy, 2015. p. 5551–58.
[15] Gudmundsson S. Sound insulation improvement of floating floors. A study of parameters. Lund Institute of Technology, Department of Building Acoustics, Report TVBA-3017, Lund, Sweden, 1984.
[16] Olsson J, Linderholt A. Force to sound pressure frequency response measurements using a modified tapping machine on timber floor structures. Eng Struct 2019;196:109343. https://doi.org/10.1016/j.engstruct.2019.109343.
[17] Jeon JY, Ryu JK, Jeong H, Tachibana H. Review of the impact ball in evaluating floor impact sound. Acta Acust United with Acust 2006;92:777–86. , https://www.ingentaconnect.com/content/dav/aaua/2006/00000092/00000005/art00014.

[18] Amiryarahmadi N, Kropp W, Larsson K. Identification of low-frequency forces induced by footsteps on lightweight floors. Acta Acust United with Acust 2016;102:45–57. https://doi.org/10.3813/AAA.918923.

[19] Brunskog J, Hammer P. Prediction model for the impact sound level of lightweight floors. Acta Acust United with Acust 2003;89:309–22. , https://www.ingentaconnect.com/contentone/dav/aaua/2003/00000089/00000002/art00014.

[20] ISO 9052–1. Acoustics – Determination of dynamic stiffness – Part 1: Materials used under floating floors in dwellings. Geneva: International Organization for Standardization; 1989.

[21] Ljunggren F, Simmons C, Hagberg K. Correlation between sound insulation and occupants' perception - Proposal of alternative single number rating of impact sound. Appl Acoust 2014;85:57–68. https://doi.org/10.1016/j.apacoust.2014.04.003.

[22] Ljunggren F, Simmons C, Öqvist R. Correlation between sound insulation and occupants' perception – Proposal of alternative single number rating of impact sound, part II. Appl Acoust 2017;123:143–51. https://doi.org/10.1016/j.apacoust.2017.03.014.